American Mineralogist, Volume 66, pages 154-168, 1981

The crystal structure of santaclaraite,[1] $CaMn_4[Si_5O_{14}(OH)](OH)\cdot H_2O$: the role of hydrogen atoms in the pyroxenoid structure

YOSHIKAZU OHASHI

Department of Geology, University of Pennsylvania
Philadelphia, Pennsylvania 19104

AND LARRY W. FINGER

Geophysical Laboratory, Carnegie Institution of Washington
Washington, D.C. 20008

Abstract

A new mineral, santaclaraite $(Ca_{0.90}Mn^{2+}_{4.04}Mg_{0.05}Fe^{2+}_{0.01})_5[Si_5O_{14}(OH)](OH)\cdot H_2O$, is triclinic with $a = 10.273(4)$, $b = 11.910(4)$, $c = 12.001(6)$Å, $\alpha = 105.77(3)$, $\beta = 110.64(3)$, $\gamma = 87.13(3)°$, $V = 1317.0(8)$Å^3; $Z = 4$ for the $I\bar{1}$ unit-cell setting. The crystal structure consists of alternating tetrahedral and octahedral layers. The tetrahedral layer is made up of infinite single chains of silicate tetrahedra with a repeat period of five tetrahedra. The octahedral layer includes rows of ten octahedra with adjacent octahedral rows displaced along their length to form bands two or three octahedra wide. As isolated units, the tetrahedral chain and octahedral band of santaclaraite are similar to the corresponding portions of the rhodonite structure. The structure of santaclaraite, however, differs in that (1) two adjacent chains (or bands) in a given layer are displaced by a half c translation, and (2) the octahedral layer is rotated by a half turn in the plane parallel to the layer with respect to the adjacent tetrahedral layer. The three roles of hydrogen as hydrogen bond, hydroxyl group, and water molecule are responsible for the above half-translation and half-rotation. Three octahedral sites, M1, M2, and M3, are essentially occupied by Mn atoms. The Ca atoms are ordered in M5, and the small amount of Mg is probably concentrated in M4. Differential thermal analysis and thermogravimetric analysis indicate that the dehydration of santaclaraite occurs at approximately 550°C.

Introduction

Santaclaraite, a new mineral from the Franciscan formation, Santa Clara County, California, is structurally related to rhodonite, babingtonite, nambulite, and marsturite (Ohashi and Erd, 1978). The mineral description is given elsewhere (Erd and Ohashi, in preparation). Santaclaraite is chemically equivalent to rhodonite plus two water molecules, $CaMn_4Si_5O_{15}$ (rhodonite) + $2H_2O$; its water content is less than that of inesite, $CaMn_{3.5}[Si_5O_{14}(OH)]\cdot 2.5H_2O$, but more than that of babingtonite, $Ca_2(Fe,Mn)Fe^{3+}[Si_5O_{14}(OH)]$, nambulite, $(Li,Na)Mn_4[Si_5O_{14}(OH)]$, and marsturite, $NaCaMn_3[Si_5O_{14}(OH)]$, another recently discovered pyroxenoid (Peacor *et al.*, 1978a).

The importance of octahedral cations in controlling the octahedral–tetrahedral linkages in the pyroxenoid structure has previously been discussed for three-tetrahedral-repeat pyroxenoids (Ohashi and Finger, 1978). The octahedral cations are identical in rhodonite and santaclaraite, so the different structures must be due to effects produced by the hydrogen atoms.

Inesite, a double-chain silicate with a five-tetrahedral repeat, has two crystal-chemically distinct types of hydrogen atoms, one as H_2O and the other as OH^- (Wan and Ghose, 1975, 1978). The hydrogen in babingtonite (Araki and Zoltai, 1972) and nambulite (Narita *et al.*, 1975; Murakami *et al.*, 1977) is believed to form a hydrogen bond O–H ··· O, on the basis of the short O–O distance, as in pectolite (Prewitt and Buerger, 1963; Takéuchi and Kudoh, 1978).

Santaclaraite is unique among pyroxenoid miner-

[1] Approved by the Commission on New Minerals and Mineral Names, IMA.

0003-004X/81/0102-0154$02.00

als in that alkali atoms such as Na and Li are not essential constituents and also in that as many as four hydrogen atoms exist for each five silicons. Thus a detailed structural analysis of this mineral should provide a better understanding of the role of hydrogen in pyroxenoid structures.

Experimental

Unit-cell setting

Crystals of santaclaraite are commonly prismatic and elongated along the zone axis of two well-developed cleavages that intersect roughly at a right angle, as in other pyroxenoids and pyroxenes. Preliminary study with precession and zone-axis photographs showed that the crystal was triclinic and that a translation along the zone of the two cleavages was approximately 12Å. This translation can be compared with the chain-identity period of five-tetrahedral-repeat pyroxenoids, rhodonite and babingtonite (Table 1). The crystallographic *c* axis is chosen parallel to the zone axis.

The (*hk*0) precession photograph, which contains information on the structure projected along the zone axis, is similar to the corresponding photograph of rhodonite. No similarities to rhodonite were observed, however, in other photographs of santaclaraite.

The unit cell of santaclaraite is compared with that of rhodonite in Figure 1. Although the B-centered cell of santaclaraite corresponds to the primitive cell

Table 1. Comparison of the unit cells for santaclaraite, rhodonite, and babingtonite

	Pyroxene-type cell			Pyroxenoid-type cell		
	STC*	RHD**	BBN†	STC*	RHD**	BBN†
Space group	$I\bar{1}$	$C\bar{1}$	$C\bar{1}$	$B\bar{1}$	$P\bar{1}$	$P\bar{1}$
a(A)	10.273(4)	9.844	9.731	15.610(4)	6.707	6.719
b	11.910(4)	10.540	10.410	7.591(2)	7.682	7.509
c	12.001(6)	12.234	12.245	12.001(6)	12.234	12.245
α(°)	105.77(3)	108.68	108.36	109.80(3)	111.54	112.21
β	110.64(3)	103.29	104.27	88.59(3)	85.25	86.25
γ	87.13(3)	82.23	84.94	99.94(2)	93.95	92.13
V(A³)	1317.0(8)	1167.7	1141.4	1317.0(8)	583.8	570.7
cleavages	$(1\bar{1}0)$ (110)	$(1\bar{1}0)$ (110)	$(1\bar{1}0)$ (110)	(100) (010)	(100) (010)	(100) (010)
tetrahedral chain	[001]	[001]	[001]	[001]	[001]	[001]
close-pack layer	(100)	(100)	(100)	(210)	(110)	(110)

* Santaclaraite. This study. From least-squares refinement with twelve reflections centered on a single crystal diffractometer.
** Rhodonite. Calculated from reduced cell data given by Peacor and Niizeki (1963)
† Babingtonite. Calculated from reduced cell data given by Araki and Zoltai (1972)

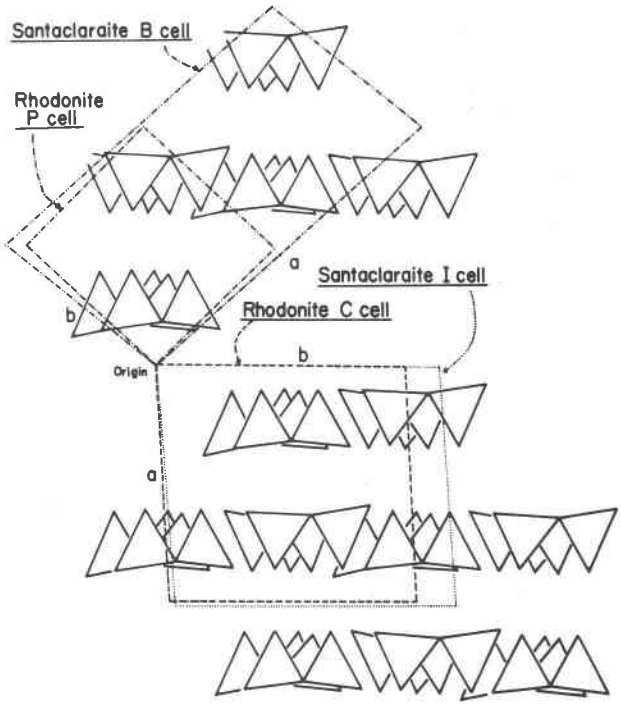

Fig. 1. Comparison of unit cells for santaclaraite and rhodonite. Triangles represent tetrahedral chains in rhodonite projected along the chain direction.

of rhodonite, it is more convenient in discussing modular crystallography (Thompson, 1978) of pyroxenoids to use a body-centered cell. This $I\bar{1}$ cell of santaclaraite is comparable to the $C\bar{1}$ setting for rhodonite and also to multiple cells for three-repeat-pyroxenoids discussed by Ohashi and Finger (1978).

The thickness of the layers, $d(100)$ of the $I\bar{1}$ or $C\bar{1}$ cell, is approximately equal in santaclaraite and rhodonite, whereas the *b* axis of the $I\bar{1}$ or $C\bar{1}$ cell, which is the separation of the tetrahedral chains or of the octahedral bands in a given layer, is much longer in santaclaraite (see Fig. 1). In the initial analysis, this longer separation was erroneously thought to be due to the presence of water molecules between the octahedral bands.

Data collection and structural analysis

A crystal 0.14 × 0.20 × 0.28 mm was used for collecting the X-ray diffraction intensities up to 65° in 2θ for Nb-filtered Mo$K\alpha$ radiation on an automated four-circle diffractometer. Integrated intensities measured with an ω–2θ scan were corrected for Lorentz and polarization effects. Absorption corrections (linear absorption coefficient 47.2 cm^{-1}) were also applied, using the numerical integration technique of

Burnham (1966a). A total of 3307 reflections with a structure factor greater than twice its estimated standard deviation was used in the structure analysis and refinement. Atomic scattering factors for the fully ionized state (except O^-) and dispersion corrections were taken from *International Tables for X-ray Crystallography, Vol. 4* (p. 99 and p. 149, respectively).

Wilson's N(Z) test strongly indicated the existence of a center of symmetry and thus a centrosymmetric triclinic space group was assumed in the subsequent structure analysis. Strong peaks, which form a nearly trigonal pattern on the (100) Patterson map of the body-centered cell, indicate the close-packed arrangement of cations and oxygens parallel to (100).

Direct methods of structure determination were first attempted. From a total of 3307 above-minimum reflections, 109 reflections with E values greater than 2.5 were used as input for a computer program SIGMA2 of the symbolic addition method (Karle and Karle, 1966). In addition to three origin-defining reflections, signs of two reflections were assigned to expand the data set of determined phases with a modified version of the tangent formula program (Brenner and Gum, 1968). Essentially three kinds of solutions were obtained: (1) the layer arrangement with no atoms on the inversion centers; (2) the layer arrangement with one atom on the inversion center; and (3) the displaced layer arrangement resembling inesite (Wan and Ghose, 1975, 1978). E maps for the first solution, calculated with approximately 500 reflections, showed an octahedral band apparently consisting of six unique octahedral positions, one of which had to be wrong because only five octahedral cations were expected from the chemical formula. Although the overall arrangement is different, as discussed below, each octahedral band would be like the one in rhodonite if the sixth peak were ignored. If the fifth peak were ignored, the band would be like that in nambulite (Narita *et al.,* 1975; Murakami *et al.,* 1977).

Between the octahedral layers there are several peaks that would be Si atoms if the structure is based on alternating tetrahedral and octahedral layers. An attempt was made to form a tetrahedral chain by connecting these Si positions and oxygens found in the octahedral layers. There were, however, no meaningful electron densities at the positions where the bridging oxygens were expected.

The computer program MULTAN of Main *et al.* (1971) was also used in an attempt to solve the structure by direct methods. All trial models were as described above. Thus, because no reasonable structure could be developed from these models, structure solution by direct methods was abandoned.

The minimum-function method was then tried using possible M–M inversion vectors. The results were essentially the same as those obtained from the direct methods: the three structural arrangements described above were also found, and the tetrahedral chain could not be located. In spite of incomplete results from the direct and minimum-function methods, however, the layer arrangement with no atoms at the inversion center seemed a plausible part of the correct structure. This optimistic view was largely based on analogy with the known crystal structures of other five-repeat pyroxenoids. The geometry of the gap between the octahedral bands, therefore, was analyzed in an attempt to fit a five-repeat tetrahedral chain. Two cases are known of octahedral–tetrahedral linkage: one in rhodonite and the other in the hydrous phases babingtonite and nambulite (Takéuchi, 1976).

Two possible arrangements for the tetrahedral chain that fills the gap between the octahedral bands in santaclaraite (Fig. 2) were derived. Both models required 17 (not 15) oxygens based on five silicons, the same number of oxygens as in the chemical formula. This result was unexpected because the independent water molecule or molecules such as those found in inesite had also been anticipated in santaclaraite.

The arrangement shown in Figure 2b yielded a residual factor, R, of 55 percent after the scale factor was adjusted. A further refinement by the least-squares method did not improve the R factor and resulted in unrealistic Si–O distances. Successive Fourier syntheses, however, improved the structural model to an R of 43 percent. The structure refinement was smooth and straightforward after this stage. Three cycles of least-squares refinement with the program RFINE2 (Finger and Prince, 1975) brought the R factor to 23, 7 and 4 percent. The final R factor is 3.6 percent for 3307 above-minimum reflections.[2] Atomic coordinates and isotropic temperature factors are given in Table 2, and interatomic distances are listed in Table 3.

Problems in nearly close-packed arrays

The process of structure analysis has been described in detail, because problems encountered with

[2] To receive a copy of the F_o and F_c table, order Document AM-80-145 from the Business Office, Mineralogical Society of America, 2000 Florida Avenue, N.W., Washington, D.C. 20009. Please remit $1.00 in advance for the microfiche.

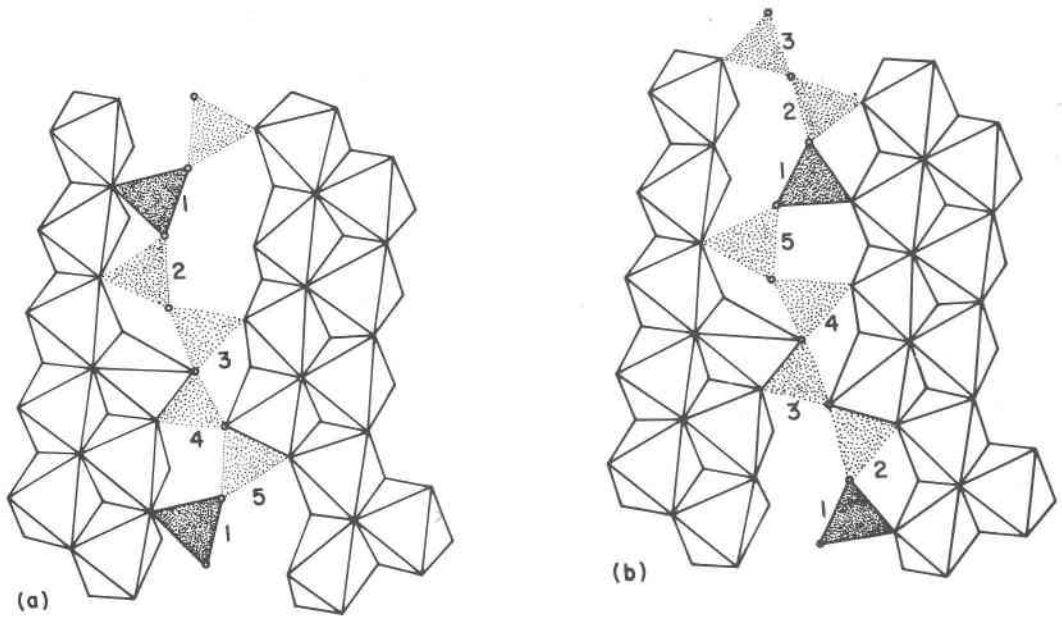

Fig. 2. Two possible arrangements of a tetrahedral chain between octahedral bands in the same layer. Note that a different location of the Si1 tetrahedron results from reversing the chain direction. Initial values of coordinates for bridging oxygens, indicated by small circles, were derived from these diagrams. The arrangement that accounts for observations for santaclaraite proved to be that shown in Fig. 2b.

santaclaraite may have general significance for analysis of a structure based on a nearly closest-packed arrangement. In such a structure there are many parallel interatomic vectors. Thus, the portion of the structure that is based on these vectors can be found on the E maps or the minimum-function maps. The first problem is the existence of false peaks at the edge of the structural unit. Although the octahedral rows end at M5 in the refined structure of santaclaraite (Fig. 4), the initial E maps contain an equally strong peak at the position where a cation would be expected if the octahedral row extended beyond M5.

A second but more serious problem is that atoms that deviate from the closest-packed array tend to be masked by strong modulation of closest-packed atoms. In santaclaraite, for example, each octahedral band can be approximated by a closest-packed arrangement, but the adjacent band in the same layer is slightly displaced and is not on the *extension* of such closest-packing. In other words, oxygens in the gap between two octahedral bands are not on the closest-packed net. Reflections that contain critical information on these "out-of-net" atoms are outnumbered in the phase determination by reflections to which mostly "on-the-net" atoms contribute, because phases for the latter group of reflections can be determined with a higher probability.

The problems in the use of direct methods of solving this structure have been studied by J. Karle, Naval Research Laboratory (personal communication, 1979). He has concluded that if six to eight symbolic phases had been used in the initial stages the correct structure would have been found.

Description of the structure

Figure 3 shows a perspective view of the basic structural units, the tetrahedral chains and the octahedral bands, both extending in the *c*-axis direction. Two tetrahedral chains cross-link two octahedral bands by sharing oxygens that are on the basal faces of tetrahedra and at the edge of the octahedral bands. The tetrahedral chains also attach, at the apical oxygens, to the central part of the octahedral bands. Therefore, a given tetrahedral chain bridges two octahedral bands in the same layer and also ties together octahedral bands in neighboring layers. The resulting structure consists of alternating arrangements of tetrahedral and octahedral layers.

The octahedral layer of santaclaraite is compared with that of rhodonite in Figure 4. Each octahedral band is remarkably similar in the two structures, but every other band in santaclaraite is displaced by a half *c* translation relative to the arrangement in rhodonite. This displacement results in a slightly wider gap between two octahedral bands in santaclaraite.

Table 2. Atomic positional parameters* and isotropic temperature factors of santaclaraite

Atom	x	y	z	B(Å^2)
M1	0.01041	0.03761	0.87646	0.64
M2	0.00534	0.11316	0.62112	0.52
M3	0.02109	0.83376	0.63081	0.62
M4	0.00166	0.24218	0.11853	0.56
M5	0.01957	0.31307	0.86949	0.70
Si1	0.2092	0.5836	0.5776	0.41
Si2	0.2203	0.6605	0.3564	0.44
Si3	0.2256	0.4693	0.1212	0.40
Si4	0.2101	0.5305	0.8810	0.40
Si5	0.1953	0.3531	0.6409	0.39
OA1	0.1270	0.8910	0.8386	0.66
OA2	0.1115	0.8140	0.0865	0.65
OA3	0.1071	0.0210	0.3269	0.62
OA4	0.1221	0.9548	0.5760	0.60
OA5	0.1366	0.1528	0.8169	0.56
OB1(OH)	0.1204	0.6740	0.6437	0.74
OB2	0.1316	0.7672	0.3327	0.73
OB3	0.1536	0.3399	0.0887	0.70
OB4	0.1363	0.6393	0.8435	0.87
OB5	0.1068	0.2307	0.5620	0.62
OC1	0.1740	0.5938	0.4398	0.72
OC2	0.1683	0.5646	0.2155	0.68
OC3	0.1602	0.5011	0.9873	0.63
OC4	0.1549	0.4076	0.7663	0.63
OC5	0.1575	0.4485	0.5603	0.67
OD1(OH)	0.1041	0.0863	0.0802	0.75
OD2(H_2O)	0.1293	0.2764	0.3267	0.90
Estimated standard errors				
M	0.00005	0.00004	0.00004	0.01
Si	0.00008	0.00007	0.00008	0.01
O	0.0002	0.0002	0.0002	0.03

* Based on $I\bar{1}$ cell (Table 1).

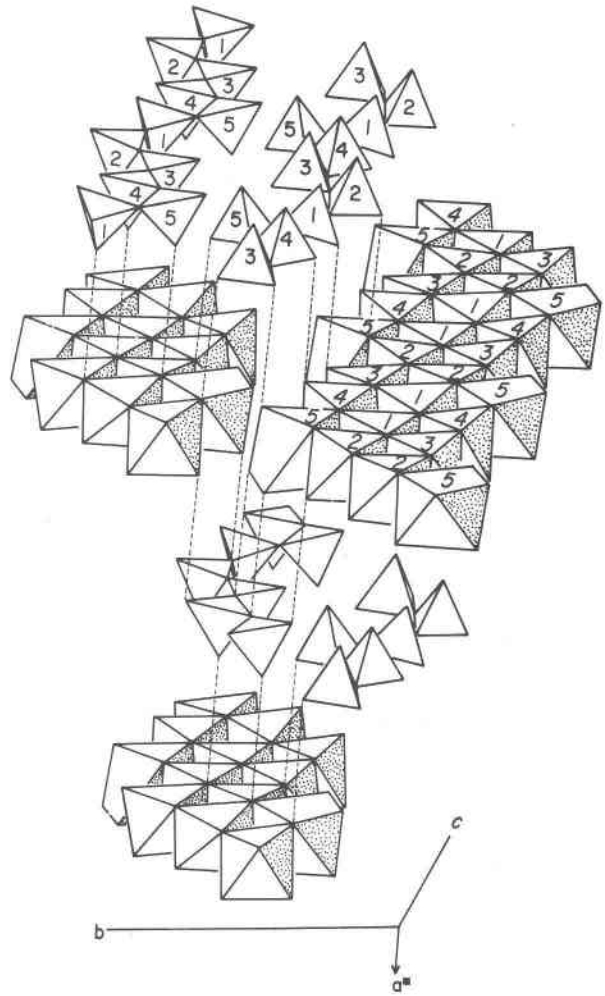

Fig. 3. A perspective view of the santaclaraite structure. Tetrahedral chains and octahedral bands are displaced along broken lines to avoid superposition.

The tetrahedral layer of santaclaraite is compared with that of rhodonite in Figure 5. The major difference in the tetrahedral chain is in the C-shaped joint formed by three tetrahedra Si1–Si5–Si4 (tetrahedral triplet), which is more open in rhodonite. Every other tetrahedral chain in the same layer is again displaced by a $c/2$ translation. The most important difference is orientation of the chains with respect to the octahedral layer next to the chain. Note the directions of the b and c axes in Figures 4 and 5. The tetrahedral layer of santaclaraite must be turned upside down in the projection plane in order to obtain the orientation found in santaclaraite with respect to the octahedral layer. If the tetrahedral–octahedral relation in rhodonite is defined as parallel, then the relation can be referred to as antiparallel in santaclaraite. The antiparallel arrangement is also found in nambulite and babingtonite. A portion of the santaclaraite structure showing the packing of octahedral bands and tetrahedral chains is given in Figure 6.

Table 3. M–O and Si–O distances* (Å) in santaclaraite

M1-	M2-	M3-	M4-	M5-
OA1 2.140	OA3 2.320	OA1 2.248	OA1 2.349	OA2 2.319
OA2 2.188	OA4 2.264	OA3 2.215	OA2 2.228	OA5 2.302
OA3 2.219	OA4 2.184	OA4 2.152	OB3 2.144	OB2 2.311
OA5 2.306	OA5 2.178	OB1 2.162	OB4 2.062	OB3 2.433
OD1 2.198	OB2 2.092	OB5 2.143	OD1 2.141	OC2 2.494
OD1 2.175	OB5 2.158	OD2 2.312	OD2 2.298	OC3 2.457
				OC4 2.599
Ave.2.204	2.199	2.205	2.204	2.416
Si1-	**Si2-**	**Si3-**	**Si4-**	**Si5-**
OA1 1.610	OA2 1.618	OA3 1.603	OA4 1.613	OA5 1.626
OB1 1.624	OB2 1.583	OB3 1.606	OB4 1.583	OB5 1.591
OC1 1.601	OC2 1.625	OC3 1.633	OC4 1.651	OC5 1.661
OC5 1.638	OC1 1.667	OC2 1.655	OC3 1.654	OC4 1.642
Ave.1.618	1.623	1.624	1.625	1.630

* Estimated standard errors for individual M-O and Si-O bonds are 0.002Å.

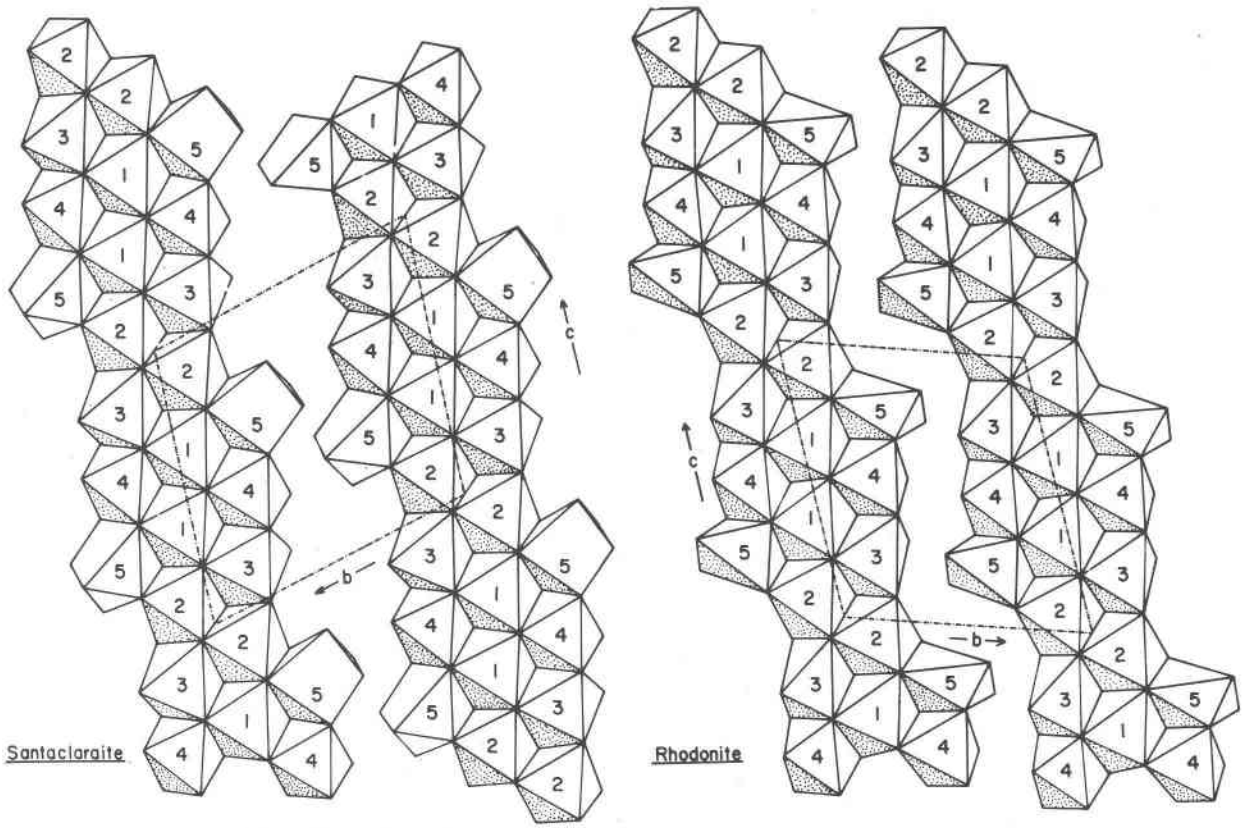

Fig. 4. Comparison of octahedral band arrangements in santaclaraite and rhodonite.

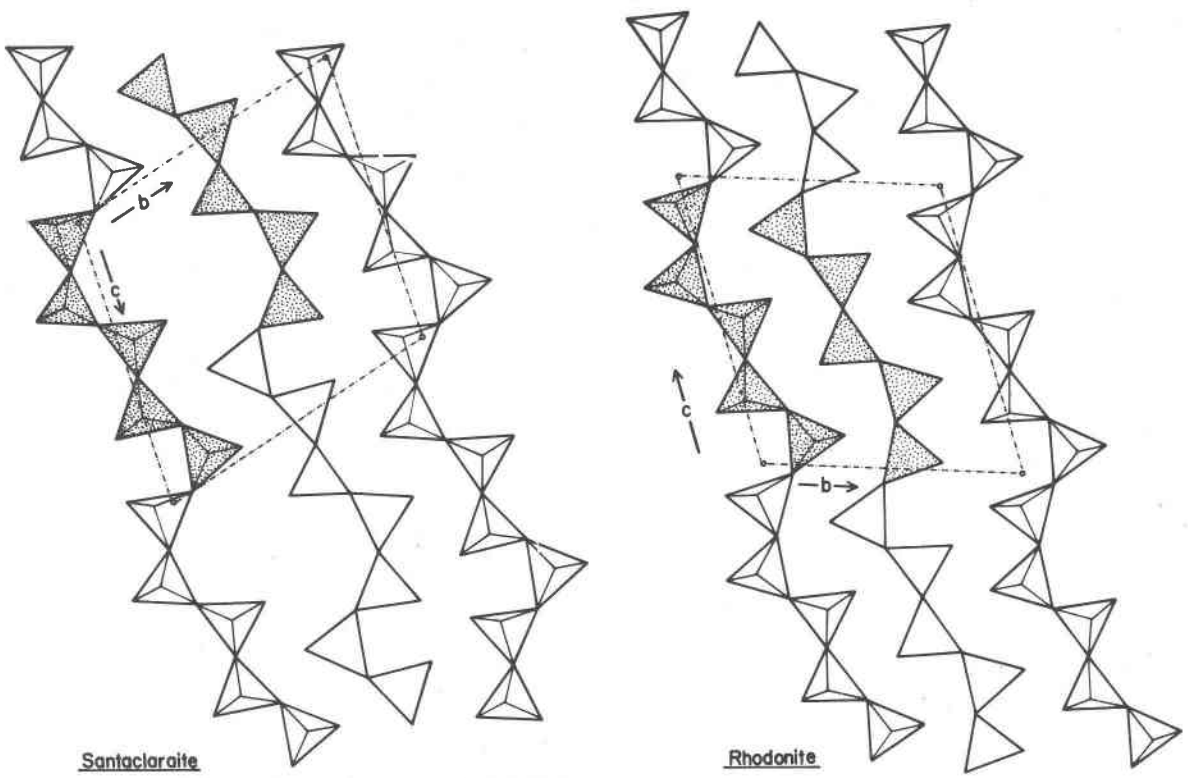

Fig. 5. Comparison of tetrahedral chain arrangements in santaclaraite and rhodonite.

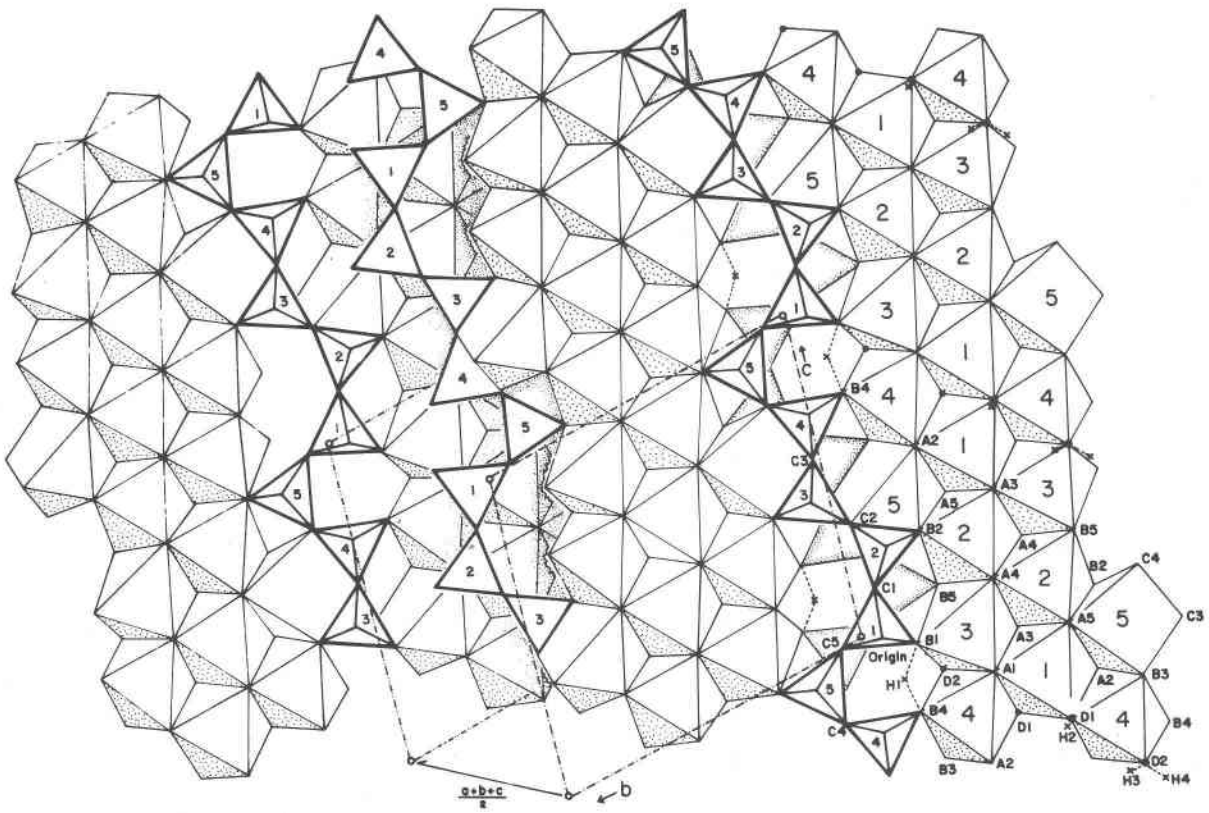

Fig. 6. A portion of the santaclaraite structure projected from the $-\mathbf{a}^*$ direction onto the close-packed layer plane. A lower layer shown on the left half of the diagram is related by a body-centering translation, $\frac{1}{2}(\mathbf{a} + \mathbf{b} + \mathbf{c})$, to an upper layer shown on the right.

Cation ordering

The coordination polyhedra for M1, M2, and M3 can be described as slightly distorted octahedra with average M–O distances of 2.204, 2.199 and 2.205Å, respectively. Refinements of cation occupancies indicate that Mn is the only cation in M1, M2, and M3 (Table 4). Coordination polyhedra (Table 3) and site occupancies are thus in good agreement for the occupancy of Mn in these three sites. The coordination polyhedron for M4 is a more distorted octahedron with a larger variation of M–O distances, ranging from 2.062 to 2.349Å (Table 3). When refined with a linear combination model of Mn^{2+} (23 electrons) and

Table 4. Cation occupancies in santaclaraite and Mg-rich rhodonites

	Santaclaraite					Mg-rich rhodonites						
	Model 1*		Model 2**			Natural			Synthetic			
	Mn	Ca	Mn	Ca	Mg	Mn	Ca	Mg	Mn	Mg	Mn	Mg
M1	1.01	-0.01	1.01	-0.01		0.89		0.11	0.696	0.304	0.615	0.385
M2	1.00	0.00	1.00	0.00		0.86		0.14	0.746	0.254	0.687	0.313
M3	0.99	0.01	0.99	0.01		0.86		0.14	0.634	0.366	0.572	0.428
M4	0.91	0.09	0.95		0.05	0.53		0.47	0.481	0.519	0.350	0.650
M5	0.14	0.86	0.09	0.91		0.40	0.60		0.868	0.132	0.876	0.124
Total	4.05	0.95	4.04	0.91	0.05	3.54	0.60	0.86	3.425	1.575	3.100	1.900
e.s.d.	0.007	0.007	0.004	0.004		0.01		0.01			0.005	0.005
Reference	This study					Peacor et al. (1978b)			Murakami and Takéuchi (1979)		Finger and Hazen (1978)	

* Linear combination of Mn and Ca with a constraint of the bulk chemical composition.
** All Mg assigned to M4 with occupancy fixed at 0.95Mn+0.05Mg.

Ca^{2+} (18 electrons), an occupancy of 0.91Mn + 0.09Ca (22.5 electrons) was obtained for M4. A more probable interpretation of the M4 occupancy, however, is to assign Mg^{2+} (10 electrons), which was not included in this stage of the refinement, to M4. When all available Mg, 0.05 cation on the basis of five cations, is assumed to occupy the M4 site in place of Ca, the occupancy would be 0.95Mn + 0.05Mg (22.4 electrons) in agreement with the total number of electrons obtained in the refinement. Thus, occupancies have been refined with that of M4 fixed at 0.95Mn + 0.05Mg (Model 2 in Table 4).

Also compared in Table 4 are the results of cation occupancy refinements in synthetic rhodonites (Finger and Hazen, 1978; Murakami and Takéuchi, 1979) and a natural Mg-rich rhodonite (Peacor *et al.*, 1978b). These studies support the preference of Mg for the M4 site, though to different degrees. The degree of ordering is less in the synthetic rhodonites, probably because the crystals were quenched from a rather high temperature (~1300°C).

The M5 coordination polyhedron in santaclaraite is extremely distorted and is almost seven-coordination, the seventh M–O distance being 2.599Å. A similar kind of distortion is found for M5 in Ca-rich rhodonite (*e.g.* Peacor and Niizeki, 1963). The cation occupancy refinement yielded 0.14Mn + 0.86Ca for M5 in santaclaraite. For both santaclaraite and rhodonite a reasonable conclusion is that most of the Ca occurs in M5 and that an apparent Ca occupancy in M4 is most probably due to the presence of a minor amount of Mg in the site.

Hydrogen atoms

In other hydrous single-chain pyroxenoids for which structures are known, there is only one hydrogen in the asymmetric unit. The hydrogen in these pyroxenoids forms a hydrogen bond between two oxygens at the open side of the C-shaped tetrahedral triplet, resulting in a slight shortening of the chain length in hydrous phases as compared with anhydrous counterparts (Prewitt and Buerger, 1963, and Takéuchi and Kudoh, 1978, for pectolite; Araki and Zoltai, 1972, for babingtonite; Narita *et al.*, 1975, and Murakami *et al.*, 1977, for nambulite).

From its chemical composition, four hydrogen atoms are expected in the asymmetric unit of santaclaraite. One of the four is probably between OB1 and OB4 as in other hydrous pyroxenoids, because the *c* length of santaclaraite is much shorter than that of rhodonite as a result of a shorter OB1–OB4 distance. All 17 oxygen atoms were found in the structure analysis, and thus the remaining three hydrogens must be bonded to some of these oxygens. There is no possibility, therefore, of the existence of an independent water molecule as in inesite and zeolites.

The anion charge determination method proposed by Donnay and Allmann (1970) has been applied to predict forms of hydrogen in the structure. The results of the calculation, shown in Table 5, indicate

Table 5. Bond valences in valence units estimated by the Donnay–Allmann method

	M1	M2	M3	M4	M5	Si1	Si2	Si3	Si4	Si5	Total	Interpretation
OA1	0.38		0.30	0.22		1.00					1.90	
OA2	0.34			0.32	0.32		1.01				1.99	
OA3	0.32	0.24	0.33					1.04			1.93	
OA4		{0.29 0.34	0.38						1.02		2.03	
OA5	0.26	0.35			0.33					1.01	1.95	
OB1			0.37			0.99					1.36	O–H···O
OB2		0.43			0.33		1.08				1.84	
OB3				0.38	0.28			1.04			1.70	
OB4				0.46					1.09		1.55	O···H–O
OB5		0.37	0.38							1.08	1.83	
OC1						1.03	1.00				2.03	
OC2					0.27		0.91	0.98			2.16	
OC3					0.27			0.94	0.95		2.16	
OC4					0.22				0.94	0.94	2.10	
OC5						0.96				0.98	1.94	
OD1	{0.34 0.36			0.38							1.08	OH
OD2			0.25	0.26							0.51	H_2O
Total	2.00	2.02	2.01	2.02	2.02	3.98	4.00	4.00	4.00	4.01		

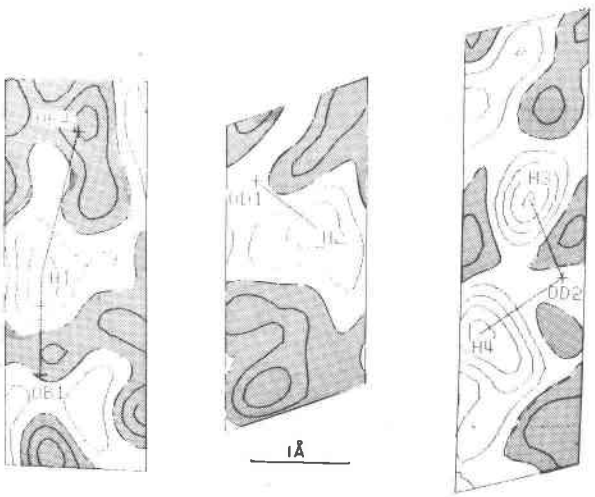

Fig. 7. Difference-Fourier maps showing possible hydrogen positions as positive residuals. Contours are at an interval of 0.2 $e/Å^3$ with the negative areas shaded.

three types of hydrogen, forming (1) O–H ··· O with OB1 and OB4, (2) O–H with OD1, and (3) H–O–H with OD2. Thermal parameters of these oxygens have been refined, using an anisotropic model to improve the difference-Fourier maps in the vicinity of hydrogen. Positive residuals in electron densities were found on the difference-Fourier maps (Fig. 7) from which coordinates for hydrogen were obtained (Table 6).

As expected, hydrogen H1 occurs between OB1 and OB4. Although the shape of the peak is somewhat irregular, H1 is closer to OB1 (0.88Å) than to OB4 (1.66Å). Takéuchi and Kudoh (1978) interpreted the difference-Fourier maps of pectolite as showing two statistically occupied hydrogen positions, O(3)–H ··· O(4) and O(3) ··· H′–O(4). In santaclaraite, however, no such second residual is found on the difference-Fourier maps. This result is consistent with the relatively large difference in bond strength between the two oxygens in santaclaraite (1.36 valence units for OB1 and 1.55 for OB4), whereas the bond strengths estimated by the Donnay–Allmann method are approximately equal for the two oxygens in pectolite.

Hydrogen H2 is bonded to OD1, forming a hydroxyl ion. Two hydrogens, H3 and H4, are approximately 1.0Å away from OD2 and make an angle of approximately 100° at OD2. In addition to these oxygens to which hydrogens are bonded, oxygen OB3, which shows a deficiency in bond strength (1.70 valence units), is only 1.72Å from H3. Oxygen OC5 is 1.83Å from H4. Thus all hydrogen atoms except H2 participate in the hydrogen bonding, as summarized in Table 6.

Oxygen atoms OD1 and OD2

The number of oxygens, including hydroxyls, in one formula unit is in general $3n$ for n-tetrahedral-repeat pyroxenoids; thus all oxygens are coordinated to silicons in order to form an infinite $(SiO_3)_\infty$ chain. Santaclaraite has, in contrast, 17 oxygens in the asymmetric unit, two of which cannot be coordinated to any of the five silicons. Atoms OD1 and OD2 are oxygens that are not bonded to silicons. These oxygen atoms are clustered near the $(01\bar{1})$ plane (shaded area in Fig. 8).

Oxygen OD1 on the upper layer in Figure 8, for example, is coordinated to three metal cations, M1, M1, and M4, which are approximately on the same level, and to hydrogen H2 directly above, forming a flattened coordination tetrahedron. A coordination around OD2 is an extremely distorted tetrahedron with two longer bonds to M3 and M4 and two shorter bonds to H3 and H4 (Table 6 and Fig. 8).

Modular crystallography

Thompson's (1978) approach to modular crystallography is here extended to a comparison of santaclaraite and rhodonite.

Tetrahedral module

Santaclaraite, $CaMn_4[Si_5O_{14} \cdot (OH)](OH) \cdot H_2O$, is chemically a hydrated equivalent of rhodonite,

Table 6. Hydrogen atoms in santaclaraite: positional parameters, bond distances and angles

*Positional Parameters**

Atom	x	y	z
H1	0.101	0.655	0.702
H2	0.181	0.089	0.116
H3	0.218	0.248	0.362
H4	0.137	0.355	0.406

Hydrogen Bonds

Donor oxygen	Hydrogen	Acceptor oxygen	Distance (A) O···O	O–H	O···H	Angle(°) O–H···O
OB1	H1	OB4	2.491	0.88	1.66	156
OD1	H2	(OD2)	2.901	0.75	(2.32)	135
OD2	H3	OB3	2.645	0.96	1.72	163
OD2	H4	OC5	2.909	1.10	1.83	164

Coordination around OD1 and OD2

Distance (A)	Angle (°)	Distance (A)	Angle (°)
OD1	H2–OD1	OD2	H3–OD2
-H2 0.75	-M1 124	-H3 0.96	-H4 99
-M1 2.197	-M1' 111	-H4 1.10	-M3 104
-M1' 2.174	-M4 117	-M3 2.312	-M4 126
-M4 2.143		-M4 2.229	
		H3	H4–OD2
		-H4 1.57	-M3 93
			-M4 130

* Obtained from difference Fourier maps.

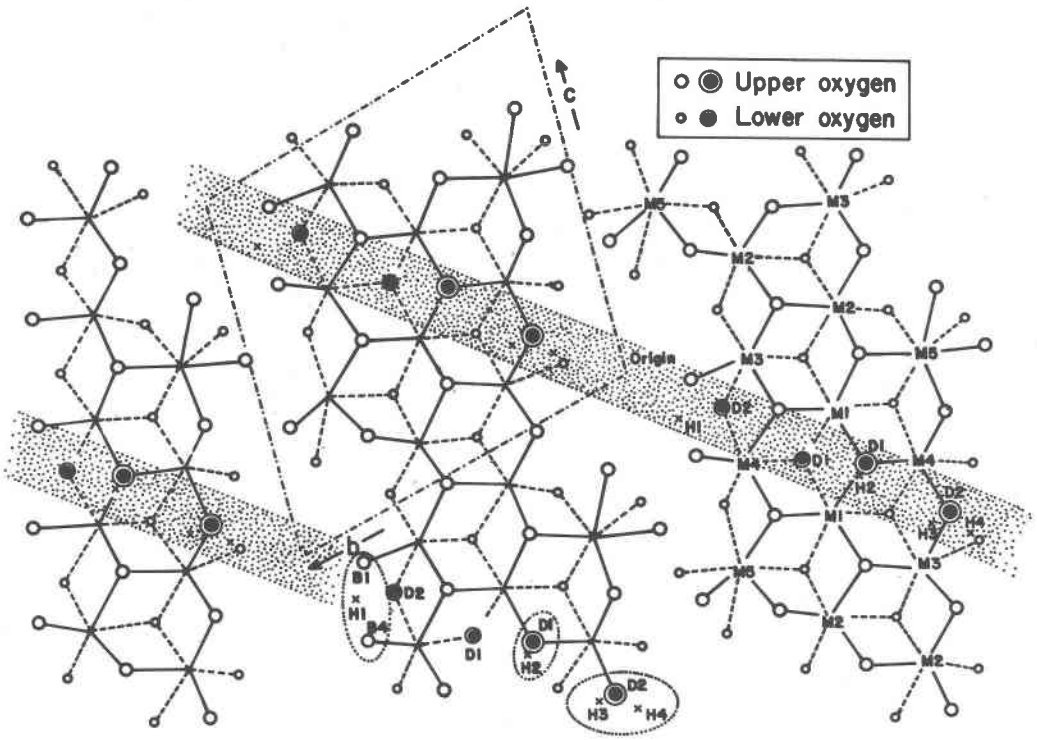

Fig. 8. Arrangement of hydrogen and oxygen atoms in the santaclaraite structure. Two layers of oxygen atoms, hydrogen atoms bonded to the *upper* oxygen atoms, and metal cations between oxygen layers are shown. Solid lines represent M–O (upper) bonds, and broken lines, M–O (lower) bonds. Three hydrogen–oxygen groups, OB1–H1–OB4, OD1–H2, and H3–OD2–H4, are indicated at the bottom. The OD1 and OD2 oxygen atoms, indicated by double circles, are arranged in the shaded area approximately parallel to the $(01\bar{1})$ layer.

$CaMn_4Si_5O_{15}$. As has been shown in the previous section, both minerals are classified as five-repeat, single-chain silicates, yet they differ in several respects. The most interesting difference is the location of the $2H_2O$ in the santaclaraite structure. A structural module that contains five tetrahedra is defined in Figure 9 to demonstrate the mechanism by which santaclaraite accommodates these additional atoms. The tetrahedral modules so defined are packed tightly in the rhodonite structure (Fig. 9a). Because the major constraint of the module arrangement is the continuity of the chains, modules could glide *lengthwise* without breaking the chains. The santaclaraite structure can be obtained when the glide operation occurs every two modules (Fig. 9b). If every module glides, the result is a hypothetical arrangement (Fig. 9c) that is an even more open structure than that of santaclaraite. Two adjacent modules of the same chain are slightly displaced at the junction of the Si1 and Si5 tetrahedra. This displacement has been called the *horizontal offset* (Burnham, 1966b) and is characteristic of pyroxenoids. There is no horizontal offset in pyroxenes.

Octahedral–tetrahedral module linkages

Each octahedral band (Fig. 4) can be taken as an infinite beam module. Santaclaraite and rhodonite have almost identical octahedral modules. The way in which octahedral and tetrahedral modules are linked should be considered. Apical oxygens of five tetrahedra form a flattened W shape (Fig. 10), each "stroke" also representing O–O edges of octahedra. There are many ways to select the positions of the W-shaped oxygen arrangement on the octahedral module. Among many possibilities are two modes of stacking (Fig. 10) that are found in santaclaraite and rhodonite. Another arrangement can be found in nambulite and babingtonite.

When only one tetrahedral chain and one octahedral band are considered, their linkage seems to be more flexible at the apical oxygens of tetrahedra than at the basal oxygens of tetrahedra (Fig. 11). Two structural constraints for the latter are the OB1–OB4 distance at the open side of the tetrahedral triplet and the distorted M5 coordination polyhedron. In santaclaraite, OB1 and OB4, bridged by the hydrogen

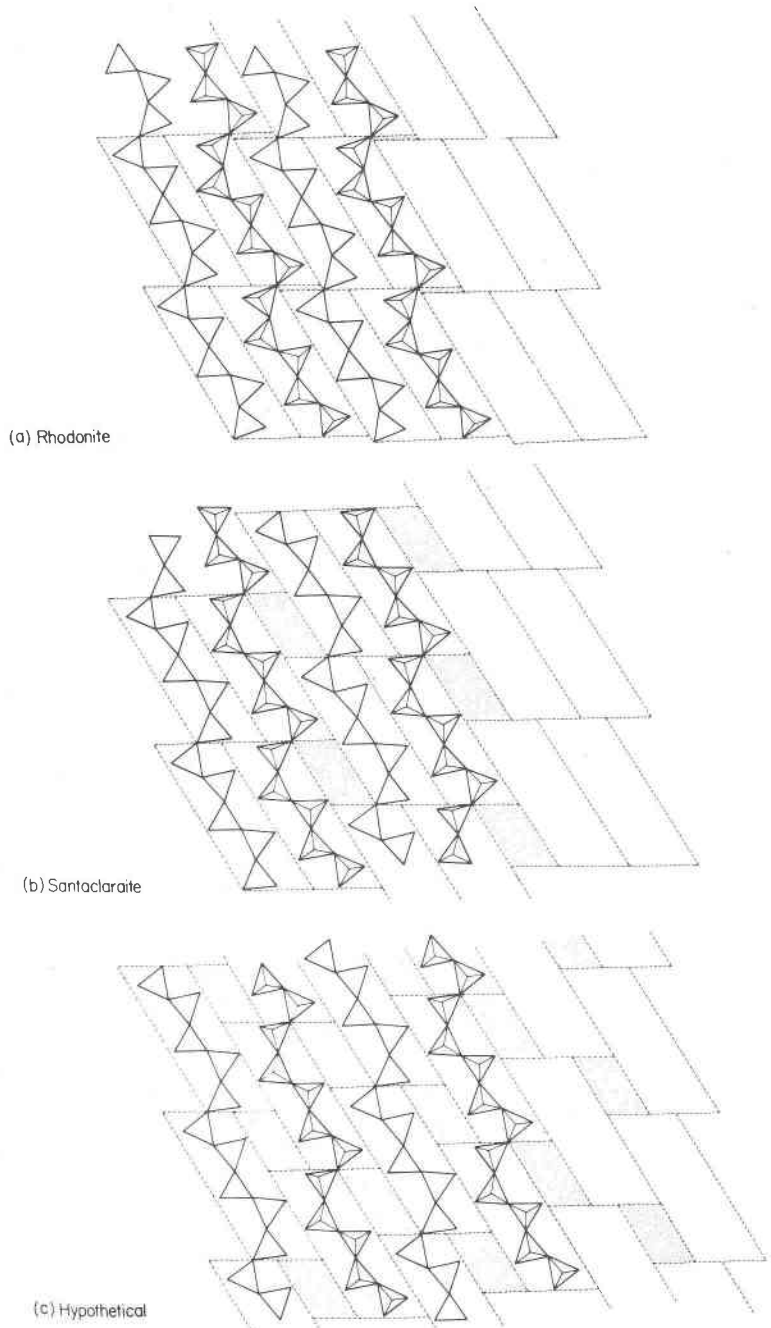

Fig. 9. Module arrangements of tetrahedral chains in (a) rhodonite, (b) santaclaraite, and (c) a hypothetical case. In santaclaraite every *other* module is displaced by half of the chain repeat length.

atom, are too close to become an edge of the Mn octahedron. Thus, the octahedral module, relative to the tetrahedral module, is arranged in such a way that these two oxygens do not coordinate to the same octahedral cation (Fig. 11a). On the other hand, the OB1 and OB4 oxygen atoms in rhodonite, which are far enough apart for an octahedral edge, are actually bonded to the same octahedral cation, M4 (Fig. 11b). A similar relationship was found in the three-repeat pyroxenoids (Ohashi and Finger, 1978, Fig. 5).

Dehydration of santaclaraite

The results of differential thermal analysis (DTA) and thermogravimetric analysis (TGA) of santacla-

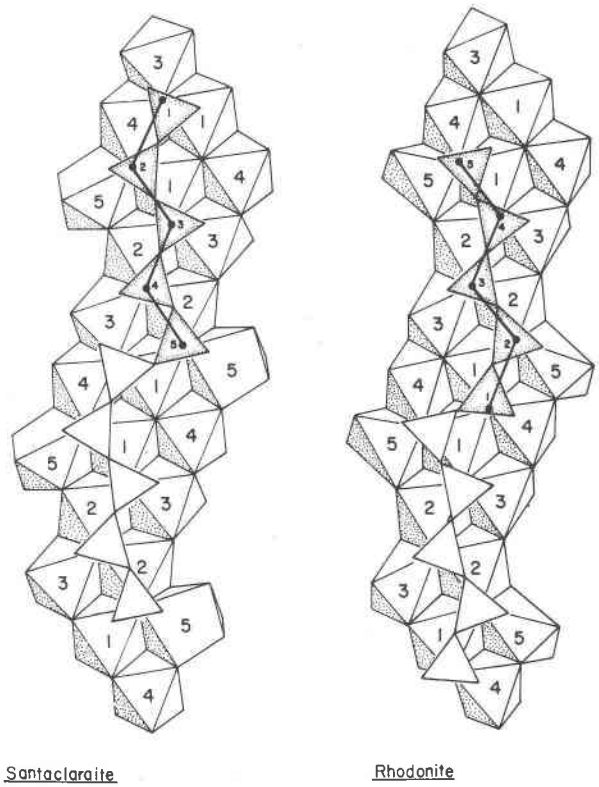

Fig. 10. Tetrahedral–octahedral linkage at the apical oxygen atoms in santaclaraite and rhodonite. The main difference between the two structures is in the position of the Si1 tetrahedron. The other four tetrahedra, though different in numbering, are similar overall.

raite are shown in Figure 12. Both show only one reaction at approximately 550°C. The reaction is endothermic, 102.3 cal/g (Gene C. Ulmer, personal communication). An X-ray powder pattern of heated santaclaraite matches that of bustamite but not that of rhodonite (Richard C. Erd, personal communication). An attempt to obtain single crystals of the high-temperature phase was unsuccessful.

The above experimental results may be interpreted as follows. Although the structural role of each of four hydrogen atoms in the asymmetric unit is not the same, dehydration of santaclaraite does not occur as multiple steps, probably because dehydration of one type of hydrogen atoms in the structure "triggers" dehydration of another. The dehydration temperature, 550°C, of santaclaraite is considerably lower than that of pectolite, 730°C (Skhirtladze, 1966). The hydrogen atom in pectolite (Takéuchi and Kudoh, 1978) is crystal-structurally equivalent to the H1 atom in santaclaraite. Dehydration of the hydrogen atoms other than H1 may cause the santaclaraite structure to become unstable, so that the H1 atom can be removed at as low a temperature as 550°C.

The direct transformation from santaclaraite to the anhydrous phase indicates that the existence of the intermediate composition, $CaMn_4[Si_5O_{14}(OH)](OH)$, is unlikely as long as the basic structure remains a single-chain silicate. Such a monohydrated form, however, might be possible if hydrogen atoms terminated silicate chains at every five tetrahedra. This hypothetical structure would be analogous to the structure of rosenhahnite, $Ca_3Si_3O_8(OH)_2$ (Wan *et al.*, 1977; Jeffrey and Lindley, 1973), which has an interrupted wollastonite-like trisilicate group:

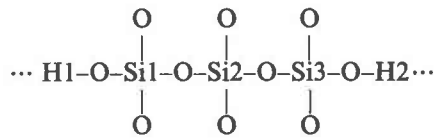

A single crystal of santaclaraite transforms when heated to multiple crystals that give only a powder X-ray pattern of bustamite. Inesite, $Ca_2Mn_7Si_{10}O_{28}(OH)_2 \cdot 5H_2O$, in contrast, was reported to transform to optically homogeneous single crystals of rhodonite when heated to 800°C (Richmond, 1942), although the exact dehydration temperature is unknown. Identification of the dehydrated inesite was, however, made with X-ray powder photographs. What causes the difference in thermal behavior between santaclaraite and inesite? One possible explanation is the difference in structure modules discussed in the previous section.

The structures of santaclaraite and bustamite are different not only in silicate chains but also in octahedral modules. In santaclaraite rows of ten octahedra form bands two or three octahedra wide (Fig. 4). The octahedral band in bustamite, on the other hand, consists of three rows of an infinite number of octahedra (*e.g.*, see Fig. 3 of Ohashi and Finger, 1978). A considerable rearrangement in the octahedral modules is required, therefore, to form the bustamite structure from santaclaraite. As a result, the dehydrated crystals do not have physical continuity controlled by an orientational relationship to the hydrated phase.

A major difference in octahedral modules between inesite and rhodonite is the length of the octahedral rows; ten-octahedral sequence of 5–4–3–2–1–1–2–3–4–5 in rhodonite *vs.* nine-octahedral sequence of 5–4–3–2–1–2–3–4–5 in inesite with M1 at the inversion center (Wan and Ghose, 1978). It is then difficult to believe that the single crystals of heated inesite obtained by Richmond (1942) were rhodonite, because

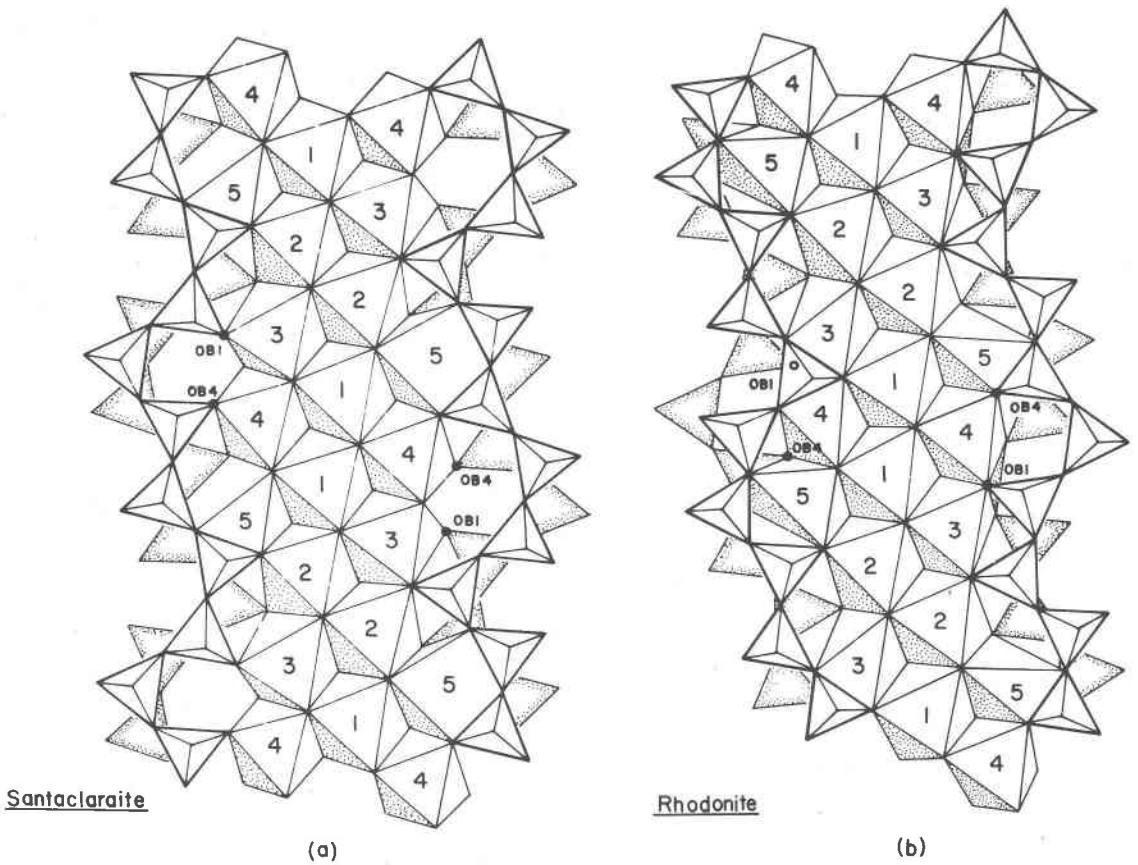

Fig. 11. Tetrahedral–octahedral linkage at the basal oxygen atoms in (a) santaclaraite and (b) rhodonite. The tetrahedral triplet Si1–Si5–Si4 has different orientations with respect to the octahedral bands. The oxygens OB1 and OB4 are coordinated to different octahedra in santaclaraite but to the same octahedron, M4, in rhodonite.

the orientational continuity of crystals could not be maintained if the octahedral modules changed their arrangement. Richmond's (1942) high-temperature phase is more likely $Ca_2Mn_7Si_{10}O_{29}$ than $Ca_2Mn_8Si_{10}O_{30}$ (rhodonite). Wan and Ghose (1978) mentioned both possibilities. If the octahedral module remains unchanged during the dehydration, the inesite transition may be regarded as gliding of the layer modules parallel to the $(\bar{2}30)$ plane. A more detailed discussion of the modular crystallography of pyroxenoids with five-tetrahedral repeats, including inesite, is in preparation.

Conclusions

The tetrahedral chain and the octahedral band in santaclaraite resemble the corresponding parts in rhodonite. A summary comparison of the two structures is given in Table 7. The hydrogen atoms play a key role in determining the unique modular arrange-

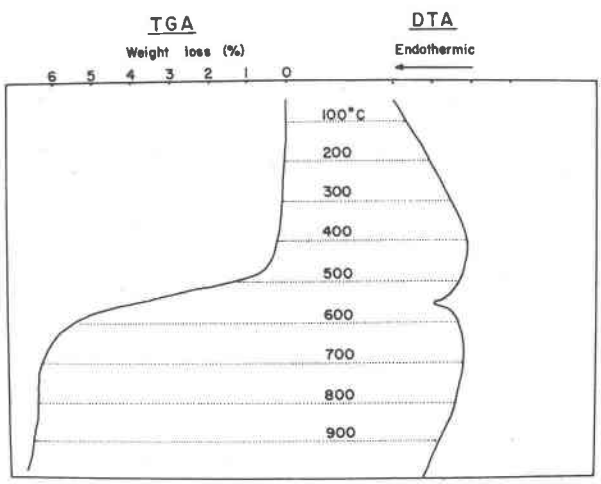

Fig. 12. DTA and TGA curves of santaclaraite. Dehydration occurs at around 550°C. Experiments were done at a rate of 10°C/min in a stream of helium with a flow rate of 3cm³/sec. The reference material used for DTA was Al_2O_3.

Table 7. Comparison of the structure modules and modular relationship in santaclaraite and rhodonite

	Beam module*	Layer module**
Tetrahedral chain	Similar. A single chain of five tetrahedral repeat. (Fig. 5)	Every other chain is displaced by ½c in santaclaraite. (Fig. 9)
Octahedral band	Similar. Rows of ten octahedra forming bands two or three octahedra wide. (Fig. 4)	Every other band is displaced by ½c in santaclaraite.
Tetrahedral-octahedral relationship	Opposite. Antiparallel in santaclaraite and parallel in rhodonite. (Figs. 10 and 11)	Opposite. Tetrahedral layers in reversed orientation with respect to octahedral layers in santaclaraite.

* Parallel to c axis of $I\bar{1}$ cell for santaclaraite and $C\bar{1}$ cell for rhodonite.
** Formed by connecting beam modules in the (100) plane.

ment in santaclaraite. The linkages of octahedral and tetrahedral modules as the *basal* oxygens of tetrahedra are controlled by the hydrogen H1, which forms the hydrogen bond at the opening of the tetrahedral triplet Si1–Si5–Si4. Furthermore, the linkage of octahedral and tetrahedral modules at the *apical* oxygens of tetrahedra is primarily affected by the existence of the hydrogens H2, H3, and H4.

As a result, adjacent tetrahedral chains (and also octahedral bands) in santaclaraite are displaced by a half *c* translation, when compared with rhodonite. This translation necessitates two more oxygens that are not connected to silicate tetrahedra and results in 17 oxygens per 5 silicons, whereas in all other pyroxenoids the ratio Si:O = 1:3 holds as a consequence of the non-existence of such oxygens.

All the hydrogen atoms in santaclaraite, despite their different structural roles, are dehydrated on heating in one continuous reaction with the maximum endotherm at 550°C. After the dehydration, single crystals are polycrystalline and have inverted to a phase that probably has the bustamite structure.

Acknowledgments

We thank Dr. R. C. Erd for providing the santaclaraite specimen and unpublished results of heating experiments; Dr. J. R. Clark for suggesting the problem and discussion; Professor G. C. Ulmer, Dr. R. Leonard, and Mr. E. Beeghe for DTA and TGA; and Dr. J. H. Konnert and Dr. J. Karle for helpful suggestions concerning the direct method. Ohashi thanks Professor F. Liebau for several hours of constructive discussions of pyroxenoid crystal chemistry, which led to the correct assignments of hydrogen atoms. Critical comments by Dr. J. R. Clark, Professor F. Liebau, Dr. H. S. Yoder, Jr., and Professor D. R. Peacor on an early draft were most helpful in improving the manuscript. The experimental part of this study was completed at the Geophysical Laboratory, and computations were carried out at the Geophysical Laboratory, Naval Research Laboratory, Lunar and Planetary Institute, and University of Pennsylvania. This study was partially supported by NSF grant EAR77-15703.

References

Araki, T. and T. Zoltai (1972) Crystal structure of babingtonite. *Z. Kristallogr., 135,* 355–373.

Brènner, S. A. and P. H. Gum (1968) The tangent formula program for the X-ray analysis of noncentro-symmetric crystals. *U.S. Naval Res. Laboratory Rep. 6697.*

Burnham, C. W. (1966a) Computation of absorption correction and the significance of end effect. *Am. Mineral., 51,* 159–167.

——— (1966b) Ferrosilite III: a triclinic pyroxenoid-type polymorph of ferrous metasilicate. *Science, 154,* 513–516.

Donnay, G. and R. Allmann (1970) How to recognize O^{2-}, OH^- and H_2O in crystal structures determined by X-rays. *Am. Mineral., 55,* 1003–1015.

Finger, L. W. and R. M. Hazen (1978) Refined occupancy factors for synthetic Mn–Mg pyroxmangite and rhodonite. *Carnegie Inst. Wash. Year Book, 77,* 850–853.

——— and E. Prince (1975) A system of FORTRAN IV computer programs for crystal structure computations. *Natl. Bur. Stand. (U.S.) Tech. Note 854.*

International Tables for X-ray Crystallography, Vol. 4 (1974) Kynoch Press, Birmingham, England.

Jeffrey, J. W. and P. F. Lindley (1973) Remarkable new silicate structure. *Nature, 241,* 42–43.

Karle, J. and I. L. Karle (1966) The symbolic addition procedure for phase determination for centrosymmetric and non-centrosymmetric crystals. *Acta Crystallogr., 21,* 849–859.

Main, P., M. M. Woolfson and G. Germain (1971) MULTAN: A computer programme for the automatic solution of crystal structures (unpublished program manual).

Murakami, T. and Y. Takéuchi (1979) Structure of synthetic rhodonite, $Mn_{0.685}Mg_{0.315}SiO_3$, and compositional transformations in pyroxenoids. *Mineral. J. (Japan), 9,* 286–304.

———, ———, T. Tagai and K. Koto (1977) Lithiumhydrorhodonite. *Acta Crystallogr., B33,* 919–921.

Narita, H., K. Koto and N. Morimoto (1975) The crystal structure of nambulite $(Li,Na)Mn_4Si_5O_{14}(OH)$. *Acta Crystallogr., B31,* 2422–2426.

Ohashi, Y. and R. C. Erd (1978) A new pyroxenoid $Mn_4CaSi_5O_{15} \cdot 2H_2O$: its structural relationship to rhodonite,

babingtonite, nambulite and marsturite (abstr.). *Geol. Soc. Am. Abstracts with Programs, 10,* 465.

——— and L. W. Finger (1978) The role of octahedral cations in pyroxenoid crystal chemistry. I. Bustamite, wollastonite and the pectolite–schizolite–serandite series. *Am. Mineral., 63,* 274–288.

Peacor, D. R. and N. Niizeki (1963) The redetermination and refinement of the crystal structure of rhodonite, $(Mn,Ca)SiO_3$. *Z. Kristallogr., 119,* 98–116.

———, P. Dunn and B. D. Sturman (1978a) Marsturite, $Mn_3CaNaHSi_5O_{15}$, a new mineral of the nambulite group from Franklin, New Jersey. *Am. Mineral., 63,* 1187–1189.

———, E. J. Essene, P. E. Brown and G. A. Winter (1978b) The crystal chemistry and petrogenesis of a magnesian rhodonite. *Am. Mineral., 63,* 1137–1142.

Prewitt, C. T. and M. J. Buerger (1963) Comparison of the crystal structures of wollastonite and pectolite. *Mineral. Soc. Am. Spec. Pap., 1,* 293–302.

Richmond, W. E. (1942) Inesite, $Mn_7Ca_2Si_{10}O_{28}(OH)_2 \cdot 5H_2O$. *Am. Mineral., 27,* 563–569.

Skhirtladze, N. I. (1966) Pectolite found for the first time in Georgia (English translation). *Dokl. Acad. Sci. USSR, Earth Sci. Section, 169,* 155–157.

Takéuchi, Y. (1976) Two structural series of pyroxenoids. *Proc. Japan Acad., 52,* 122–125.

——— and Y. Kudoh (1978) Hydrogen bonding and cation ordering in Magnet Cove pectolite. *Z. Kristallogr., 146,* 281–292.

Thompson, J. B. (1978) Biopyriboles and polysomatic series. *Am. Mineral., 63,* 239–249.

Wan, C. and S. Ghose (1975) Inesite, $Ca_2Mn_7Si_{10}O_{28}(OH)_2 \cdot 5H_2O$: a new chain silicate with "Fünferdoppelketten." *Naturwissenschaften, 62,* 96.

——— and ——— (1978) Inesite, a hydrated calcium manganese silicate with five-repeat double chains. *Am. Mineral., 63,* 563–571.

———, ——— and G. V. Gibbs (1977) Rosenhahnite, $Ca_3Si_3O_8(OH)_2$: crystal structure and the stereochemical configuration of the hydroxylated trisilicate group, $[Si_3O_8(OH)_2]$. *Am. Mineral., 62,* 503–512.

Manuscript received, March 3, 1980;
accepted for publication, May 8, 1980.